WATER RESOURCES RESEARCH, VOL. 37, NO. 12, PAGES 3371–3381, DECEMBER 2001

Identifying eroding and depositional reaches of valley by analysis of suspended sediment transport in the Sacramento River, California

Michael Bliss Singer and Thomas Dunne

Donald Bren School of Environmental Science and Management, University of California
Santa Barbara, California, USA

Abstract. Spatial patterns in suspended sediment transport and storage along the Sacramento River were assessed by evaluating the suspended sediment budget for the main channel accounting for all tributaries and diversions. Time series analysis was employed to quantify the relationship between streamflow and suspended sediment concentration for gauging stations along the main channel and signature tributaries. Sediment concentration records (of 2-yr duration) were extended using Box-Jenkins transfer function models to calculate annual rates of suspended sediment discharge over a 32-year period since dam construction on the Sacramento River. The suspended sediment budget was evaluated to identify reaches of net erosion or deposition. The results of the budget suggest the influence of tectonics and anthropogenic channel modification.

1. Introduction

The morphology of a river is determined by the interaction of water and sediment within a channel network as the river deposits and remobilizes sediment along its valley floor. The mass balance resulting from these transport processes indicates the accumulation and removal of sediment and, in turn, determines the channel and floodplain morphology, which are reflected in flood conveyance capacity, stability of natural and engineered river courses, and the complexity of river channel and riparian habitat [*Dunne*, 1988; *Kondolf and Wolman*, 1993; *Kondolf*, 1995a; 1995b]. This paper reports an empirical investigation of decadal patterns in the disposition of suspended sediment in the channel and valley floor of the Sacramento River system.

In the last 150 years the Sacramento River has been the object of a number of anthropogenic alterations including the delivery of hydraulic mining sediments, the emplacement of an extensive system of flood control levees, and the construction of dams on the main stem and its tributaries. Although the impact of hydraulic mining sediments is still evident on one Sacramento tributary [*James*, 1991], its effect on the river bed of the lower Sacramento has long since passed [*Meade*, 1982]. However, other human modifications, including artificial levees and bank protection, have been shown to have lasting effects on the sediment budget in fluvial systems [*Kesel et al*., 1992]. The purpose of this study was to construct a suspended sediment budget for the Sacramento River valley over a recent period of decades since dam construction and to identify reaches and causes of net erosion or deposition.

2. Sources of Data

This study focuses on the analysis of suspended load which is calculated using sediment concentration data collected regularly by the United States Geological Survey (USGS) at their gauging stations. These data are collected, compiled, and processed by standardized procedures outlined by *Guy and Norman* [1970] and *Porterfield* [1972] and are published as daily mean concentrations in annual USGS Water Resources Data reports.

Suspended load error estimates inherent in USGS data collection and processing procedures have been estimated at 5% for the Colorado River and 20% for the Little Colorado River [*Topping et al*., 2000]. We acknowledge that there may be a significant amount of uncertainty in these data sets, but they remain the best data available. We utilize USGS suspended sediment concentration and daily discharge data herein to develop time series models at various gauging points and to subsequently analyze long-term patterns in sediment transport.

3. Relating Discharge to Sediment Concentration

Long-term loads of suspended sediment are usually computed from irregular, sparse measurements of sediment concentration, a relationship between concentration and water discharge determined by least squares regression [*Loughran*, 1976], and a longer record of flow. Sediment rating curves, as the regressions are called, have thus been used for predicting the sparsely collected variable, sediment concentration, based on the more frequently recorded one, streamflow. However, for a given value of flow in such a model, sediment concentration values may range over 2 orders of magnitude (Figure 1). Generally, this may be the result of hysteresis, caused by differences in sediment supply or hydraulics between rising and falling discharge and/or of variability in rainstorm characteristics and drainage basin condition. In any case, the rating curve drastically underestimates many of the highest sediment concentration peaks (those assumed responsible for the majority of suspended sediment transport) and overestimates the sediment concentration of dilute flows, even after bias corrections [e.g., *Ferguson*, 1986] are made for the regression parameters.

Most importantly, standard sediment rating curves developed using data collected over a regular time interval (e.g.,

Paper number 2001WR000457.
0043-1397/01/2001WR000457$09.00

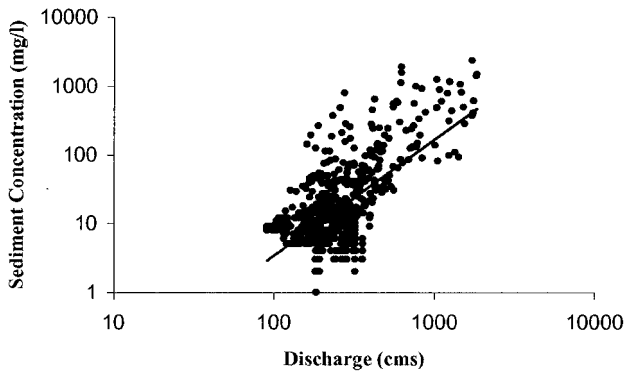

Figure 1. Sediment rating curve for Bend Bridge 1977–1980.

daily data) violate the assumption of independence and identical distributions in statistical regression, because the observed values of a particular variable are related to one another by time. Accordingly, each discharge sediment concentration data pair will plot close to the previous pair. As a result, the residuals of this type of model will be serially correlated inducing bias in the estimation of regression parameters [*Neter et al*., 1983]. This fact undermines the efficacy of the sediment rating curve for assessing long-term suspended sediment discharge and for making inferences on modes of sediment transport. Inadequacies of sediment rating curves have been recognized by previous workers, who have attempted to modify, analyze, or recreate them to account for the inconstancy in the relationship between sediment concentration and discharge [*Heidel*, 1956; *Walling*, 1977; *Ferguson*, 1986; *Marcus*, 1989; *Williams*, 1989].

In addition, the rating curve is a static model that is unable to represent the changing, in-channel conditions of fluvial sediment arising during and between high flows. It is the structure and sequencing of these events which govern sediment transport over the long term. Thus whether making long-term predictions of sediment discharge or attempting to gain insight into in-stream sediment transport processes, shortcomings in the rating curve technique make an alternative approach based on time series preferable where adequate data are available.

Previous applications of time series analysis to concentration-discharge relationships have included modeling sediment yield [*Sharma et al*., 1979; *Sharma and Dickinson*, 1980], analyzing the effect of drainage basin characteristics on suspended sediment transport [*Fitzgerald and Karlinger*, 1983; *Lemke*, 1991], and determining dominant variables controlling sediment concentration [*Rodriguez-Iturbe and Nordin*, 1968]. Employed in the present research context, this family of models (autoregressive integrated moving average models or ARIMA models) recognizes that discharge on a particular day is related to that of the previous day(s) and that sediment concentration is related to discharge on that day and previous days, as well as to previous values of sediment concentration. Such a model structure is consistent with field observations and theories of sediment supply and transport processes [*Lemke*, 1991]. Because time is included in the model structures, there is no consistent underprediction or overprediction as an artifact of hysteresis. Consequently, time series model residuals are not serially correlated.

4. Basin Characteristics

The Sacramento River drains the northern part of the Central Valley of California and has a total drainage area of 6.8×10^4 km^2 comprising over one half of the total drainage area of the San Francisco Bay system [*Porterfield*, 1980]. It flows on a subsiding alluvial base that it has deposited as the surrounding mountains have been uplifted [*Bryan*, 1923]. The river drains the 96 km wide $\times$ 418 km long Sacramento Valley, a broad, alluvial, structurally controlled lowland basin between the Sierra Nevada Mountains and the Coast Range [*Harwood and Helley*, 1987].

The river flows from its source near Mount Shasta through one structurally controlled, incised reach (Sacramento Canyon) and an entrenched, upland valley reach (hereafter referred to as the Redding Plain) and into another incised reach (Iron Canyon) on a bed of mixed gravel and sand [*Bryan*, 1923]. Downstream of Bend Bridge (Figure 2), the river enters the synclinal trough known as the Central Valley, where it assumes the character of an alluvial channel, alternating between active meandering, braided, and straight sections, building bars on an armored bed of coarse and medium gravel with a subarmor layer of coarse and medium sand. The channel lies between discontinuous high floodplain surfaces composed of fine sands, silts, and clays [*Brice*, 1977; *Water Engineering Technology* (*WET*), 1990]. Between Bend Bridge and Butte City (Figure 2) the riverbed is composed of coarse-, medium-, and fine-sand layers overlain by lobes of fine and medium gravels. The river becomes rapidly depleted of gravel in the low-gradient reach upstream of Colusa Weir (Figure 2) and transitions to a completely sandy bed between Colusa and Knights Landing [*WET*, 1990]. Finally, the Sacramento River enters the tidal zone at Sacramento [*Goodwin and Denton*, 1991].

The basin contains dams, levees, dikes, and gravel mining operations, which affect the geomorphic character of the river and its floodplain. In the 150 years since the discovery of gold in the Sierra Nevada the Sacramento River valley has been transformed by agriculture and human settlement and thus by radical flood control policies intended to ensure the survival of these floodplain activities. The flood control system was designed to convey water and sediment as efficiently as possible through the main stem Sacramento River using straightened channels and high levees built upon protected river banks to prevent overbank flooding and bank erosion and therefore lateral channel migration. To relieve pressure on the channel banks, flood waters overflow into two major flood bypasses, Sutter and Yolo, via a system of weirs which were constructed to convey water into existing lowland flood basins (Figures 2 and 3). These floodways divert water in high flows and provide multiuse zones of agriculture and habitat in drier seasons.

5. Model

The model used in this research is the Box-Jenkins transfer function model (hereafter referred to as BJ), which in this case relates inputs of streamflow to outputs of sediment concentration. The relationship between discharge and sediment concentration is a unidirectional one that can be modeled by a combination of moving average and autoregressive processes. Sediment concentration at time t (days) is a function of discharge on that day and previous days (a moving average process, referred to below as MA), as well as a function of sediment concentration on earlier days (an autoregressive process, referred to below as AR). The moving average terminology is

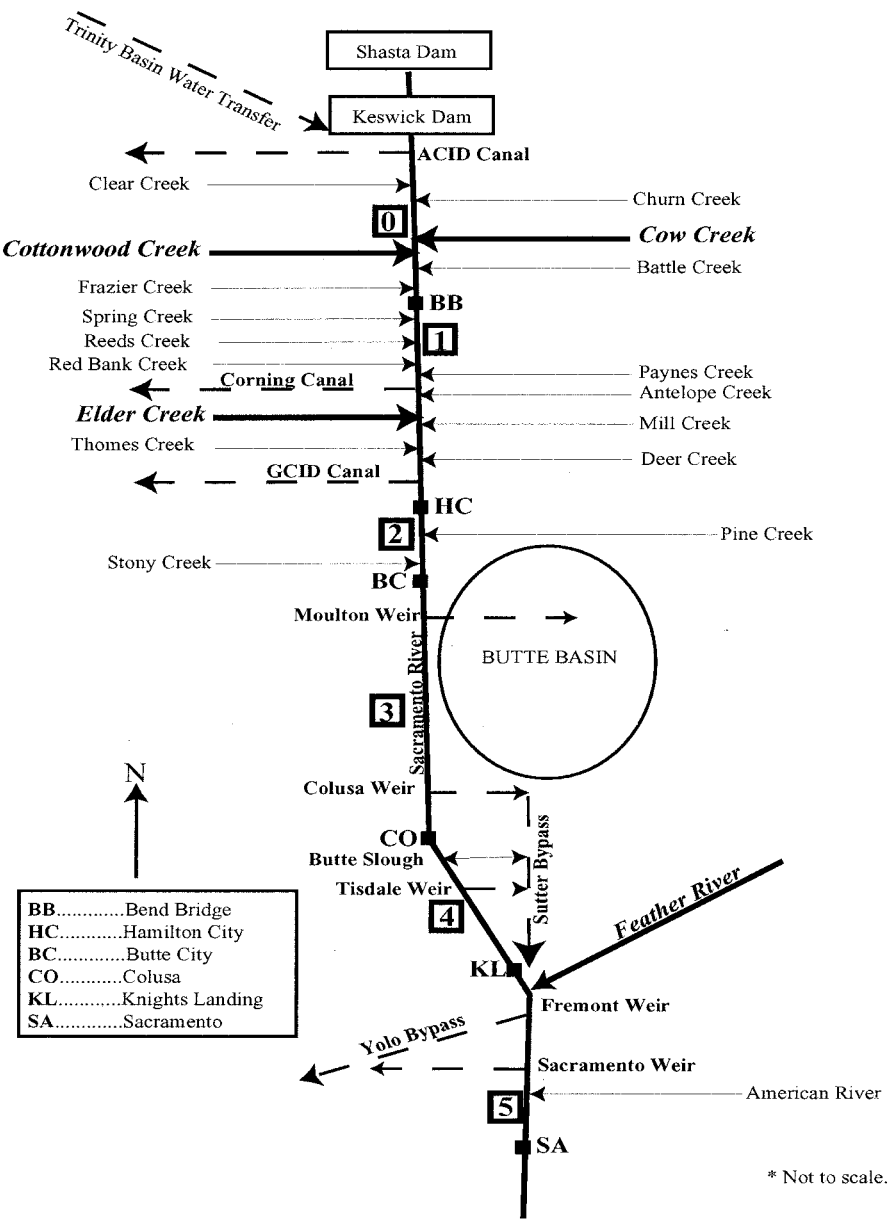

Figure 2. Schematic of tributaries, diversions, and bypasses along the Sacramento River's main channel. Project levees (not shown) begin between Hamilton City and Butte City. Artificial channels are depicted with dashed lines, and natural channels are depicted with solid lines. Gauging station names are abbreviated in bold caps. Reaches used for analysis are represented by boxed numbers.

misleading, but it is in common use [*Box and Jenkins*, 1994] and therefore is employed here. To illustrate a practical BJ example, a mixed model (i.e., both second-order MA and AR terms) can be represented in algebraic notation:

$$Cs_t - \delta_1 Cs_{t-1} - \delta_2 Cs_{t-2} = \omega_0 Q_t - \omega_1 Q_{t-1} - \omega_2 Q_{t-2}, \quad (1)$$

where Cs_t is the output sediment concentration at time t in days; Q is the input stream discharge at time $t - z$, where z represents a backward time lag; δ_r is the AR operating on previous values of sediment concentration, where r is the order of the AR (in this case $r = 2$, indicating a second-order AR); and ω_s is the MA operating on current and previous values of discharge, where s is the order of the MA (in this case $s = 2$, indicating a second-order MA). Solving for Cs_t gives sediment concentration on a particular day as a function of discharge on that day and the previous 2 days, as well as of sediment concentration on the previous 2 days. This same model can be written using the back shift operator notation:

$$(1 - \delta_1 B - \delta_2 B^2) Cs_t = (\omega_0 - \omega_1 B - \omega_2 B^2) Q_t. \quad (2)$$

In this case, B is the back shift operator such that $B^z Q_t = Q_{t-z}$. The general BJ model then appears as

$$Cs_t = \frac{\omega(B)}{\delta(B)} Q_{t-d} + e_t, \quad (3)$$

where $\omega(B) = (\omega_0 - \omega_1 B - \omega_2 B^2 - \cdots - \omega_s B^2)$ and $\delta(B) = (1 - \delta_1 B - \delta_2 B^2) - \cdots - \delta_r B^r)$; s and r are the

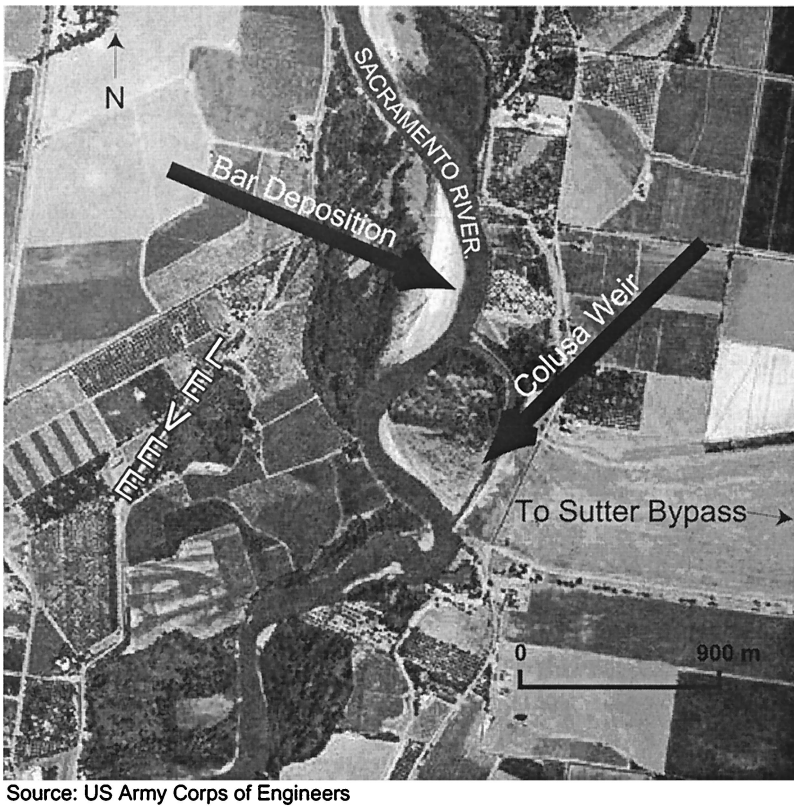

Figure 3. Aerial photograph showing Colusa Weir overflow to Sutter Bypass and point bar deposition in the wide reach-of-valley upstream (reach 3).

orders of the MA and AR, respectively; ω_s and δ_r are the estimated model parameters; and e_t is a noise process at time t, which is independent of the input and can be represented as an ARIMA process [*Box and Jenkins*, 1994]. The d parameter represents a universal lag between the response of sediment concentration to fluctuations in discharge. The delay parameter d was found to be zero for all stations on the Sacramento, so it will be excluded from further discussion.

The first term on the right side of (3) is called the systematic term and contains a transfer function consisting of weighted parameters, which determine the extent to which Cs_t depends on previous Q_t values and previous Cs_t values. Numerator parameters $\omega(B)$ in this model represent MA, whereas denominator parameters $\delta(B)$ represent AR. If an estimated model results in a strictly autoregressive BJ model (only denominator parameters), sediment concentration on a given day is predicted as a function of that day's discharge and sediment concentration from previous days. On the other hand, if an estimated model results in a strictly moving average BJ model (only numerator parameters), sediment concentration on a given day is predicted using only discharge values from that day and previous days, irrespective of previous conditions of sediment concentration (no memory). The other term in the BJ model is called the noise term and is modeled independently by an autoregressive/moving average process similar to that mentioned for the systematic term. The noise term represents the model and measurement errors.

Success in estimating BJ model parameters necessitates that the sediment concentration-discharge data are collected with frequency high enough to capture rising and falling patterns. This frequency is reasonable in large river systems (e.g., Sacramento River) where data are recorded as daily mean concentrations but may require more frequent sampling in smaller, swifter river systems. In such systems, patterns of sediment concentration as a function of discharge may be obscured by daily mean concentration-discharge data. Nevertheless, we have used such data (the best published data) in model development to obtain sediment discharges for tributaries to the Sacramento River. On the basis of the results for these models (section 7) these tributaries are large enough to model using daily data.

6. Model Application

We employed BJ models to extend daily records of sediment concentration at six main stem gauging stations and four tributary gauging stations (Figure 2) in order to calculate long-term sediment discharge at each gauging point. We used this information to evaluate the suspended sediment budget in the main stem Sacramento River in a 32-year period since construction of Shasta Dam and subsequently to identify main stem river reaches of net long-term erosion or deposition.

In this study we are providing a new level of insight into sediment transport in the Sacramento River in the form of a suspended sediment budget. An earlier total-load budget for the Sacramento River channel [*U.S. Army Corps of Engineers*, 1983] analyzed the effects of a proposed bank protection program on sources of sediment for a 19-year period. The study utilized a combination of rating curves (i.e., stream discharge versus sediment discharge), a sediment routing model, and a

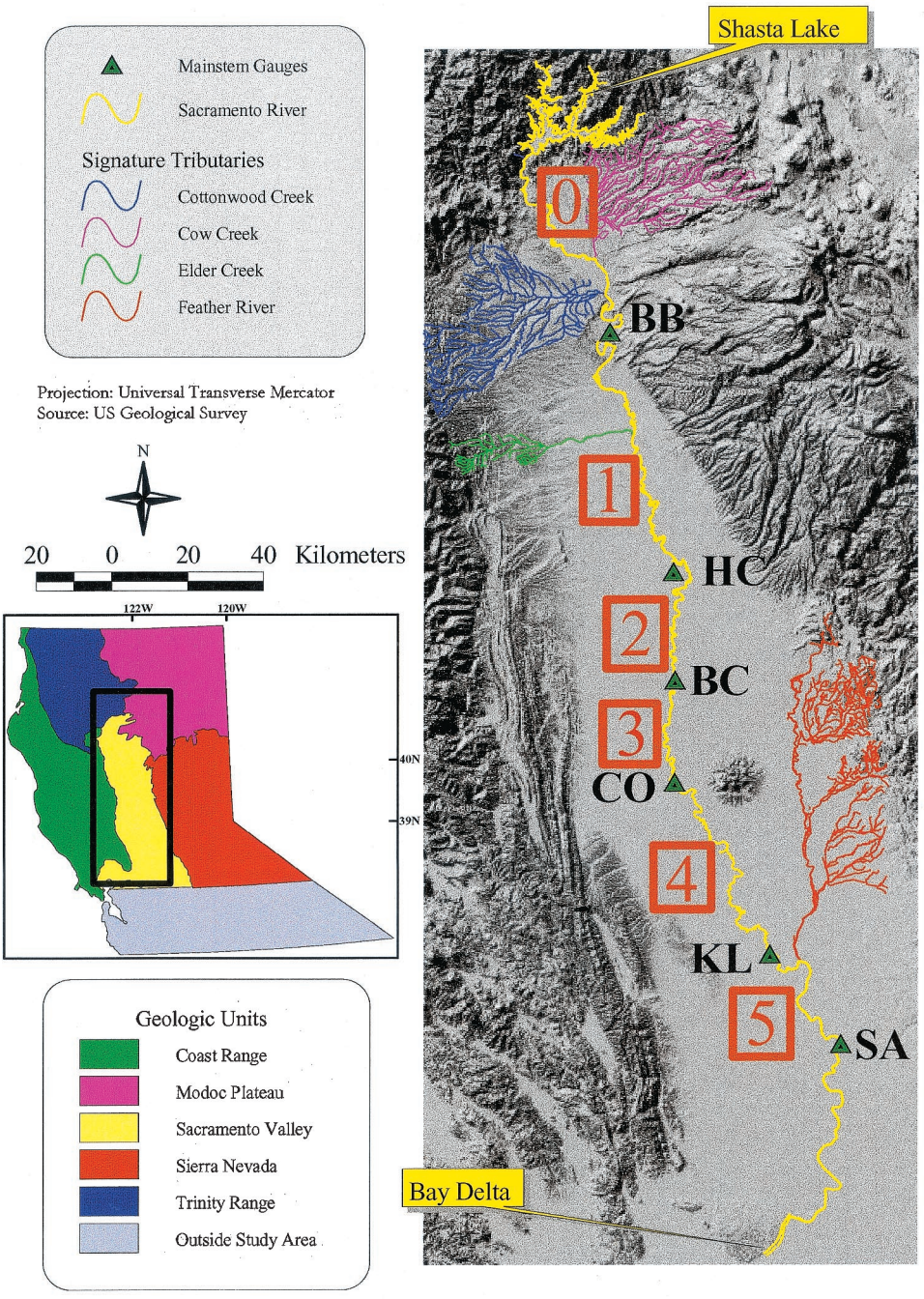

Plate 1. The Sacramento River Valley map showing the six gauging stations (triangles) used in this study, the signature tributaries (color coded), and the five reaches (boxed red numbers). The inset shows geologic units (color coded) from which signature tributaries were selected. Abbreviations for sampling stations are given in Figure 2.

priori assumptions to assess the relative importance of particular sediment sources in the system before and after project implementation. The results of the U.S. Army Corps of Engineers study will not be compared to the results in this paper because the results of its computed suspended load are not reported independently of the total-load budget results.

Other studies have alluded to a long-term trend (decrease) in sediment discharge in the Sacramento River [e.g., *Gilbert*, 1917], but our test for stationarity over the 17-year period (1963–1979) of continuous record at Sacramento revealed no temporal trend in annual suspended load ($R^2 = 0.095$ and $p = 0.229$). This result corroborates that of another study, which found stationarity in the data set [*Goodwin*, 1982].

Plate 1 shows the study reach of the main stem Sacramento River, the main stem gauging stations for which long-term sediment discharge was calculated (triangles), the main stem reaches that were evaluated for net long-term erosion or deposition (boxed numbers), and the signature tributaries (defined below and indicated in color) used to calculate sediment discharge into the Sacramento from tributary sources.

6.1. Signature Tributaries

Very few continuous suspended sediment records exist for Sacramento River tributaries. Therefore we estimated the sediment discharge from all tributaries draining a common geologic substrate using a single "signature" tributary. The Sacramento River tributaries flow from four primary geologic units (Plate 1 inset): the Modoc plateau, a volcanic lava flow in the northeast; the Sierra Nevada Mountains, a granitic batholith in the east; the Coast Range, a mélange of graywacke, shale, limestone, chert, and mafic rocks in the west; and the Trinity Mountains, a collection of granites and metavolcanic rocks in the northwest [*California Department of Water Resources*, 1994].

Each of these four units is assumed to represent a distinct sediment discharge signal based on geological substrate properties (relevant even in valley deposits below mountain fronts) and slope. Within each geologic unit the gauging station with the longest continuous record of flow and sediment concentration was designated as a signature station. Explanation of the use of signature stations to model sediment discharge follows in section 6.4.

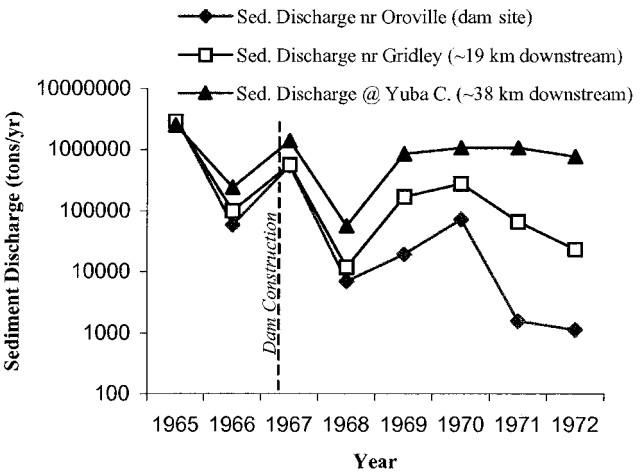

Figure 4. The annual sediment discharge before and after the construction of Oroville Dam on the Feather River, demonstrating that the dam has had minimal influence on the sediment discharge near the Feather's confluence with the Sacramento.

6.2. Temporal Domain

We developed a suspended sediment budget for the water years (WY) 1948–1979, using sediment concentration data collected at 10 gauging stations (six main stem and four tributary) between 1977 and 1979. The model for the Sacramento gauging station, however, was developed using 17 years of continuous sediment concentration data that exist for this station. We first developed BJ models relating sediment concentration to discharge for this period and then simulated long-term suspended sediment discharge for each main stem and signature station over the 32-year discharge domain common to all stations (i.e., WY 1948–1979). This method ensures the resulting sediment budget is consistent for all stations over the temporal modeling domain.

This 32-year period corresponds to the continuous historical daily hydrological record at the station of Sacramento used here as the hydrological domain of the study (the shortest hydrologic record common to all stations modeled). This period also coincides approximately with the time since the construction of Shasta Dam, the last known major perturbation on the main stem. Although there have been other engineering projects in the basin since the dam was constructed in 1945 (e.g., interbasin water transfers, in-stream gravel mining, and dam construction on tributaries) [*California Department of Water Resources*, 1994], their influence on the relationship between sediment concentration and discharge in the main channel is discounted as follows.

An interbasin water transfer from Trinity River basin, which began in 1963, increased mean annual flow at Bend Bridge by 15% but has had no significant impact on flood flows [*California Department of Water Resources*, 1994], which dominate the transport of suspended sediment. Although the removal of gravel results in temporary suspension during mining operations, it would have minimal influence on bed material suspendibility by flow over the long term. Dam construction on tributaries in the Sierra Nevada (e.g., Oroville Dam on Feather River) is assumed to have only a diffuse (or second order) effect on the sediment concentration-discharge relationship at the point of confluence with the Sacramento River because of the following: (1) Sediment yields have been low above Sierra dam sites since the last episode of glacial scour in the Pleistocene (evident in low sedimentation rates into Sierra reservoirs reported by *Dendy and Champion* [1978]). (2) There is significant sediment contribution from tributaries below impoundments which are fed by their own undammed tributaries and which cross the Sierra foothills and lowlands across valleys containing hydraulic mining tailings, agricultural lands, and other sources of alluvial sediment deposited during the Tertiary and Quaternary periods. It is unlikely that impoundments cause a large reduction in sediment discharge at the point of confluence with the Sacramento River, although they do alter the flow structure. Analyzing sediment discharge data collected before and after the construction of Oroville Dam on the Feather River lends credence to our assumption (Figure 4). Herein we consider only tributary drainage areas downstream of impoundments to calculate sediment discharge.

6.3. BJ Model Estimation Procedure

Since this study is concerned with the application of time series models to sediment budget evaluation, only an outline of time series model building is given below. For a more detailed description of algorithms and diagnostics involved in transfer function model estimation, the reader may consult *Box and Jenkins* [1994] for the general case and *Fitzgerald and Karlinger* [1983] and *Lemke* [1991] for application to sediment concentration.

To satisfy assumptions of normality, the original discharge and sediment concentration data were transformed to logarithms because discharge values were highly right skewed. BJ modeling assumes the process being investigated is stationary. A check of the correlogram of the log-transformed series of both flow and sediment concentration revealed nonstationarity (i.e., their autocorrelations did not die out to white noise with increasing lags). Therefore differences between the logarithms of successive daily flow values were used as a second transformation to convert the nonstationary series to a stationary one. Using differenced input and output data in (3) signifies that the BJ model predicts changes in sediment concentration based on changes in discharge and previous changes in sediment concentration. The original data can be retrieved at the end of the differencing procedure.

A univariate ARIMA model was then fit to the input series (i.e., log-differenced discharge) with an equation of the form:

$$Q_t^{**} = \Phi_1 Q_{t-1}^* + \cdots + \Phi_p Q_{t-p}^* + a_t - \theta_1 a_{t-1} - \cdots - \theta_q a_{t-q}, \quad (4)$$

where Q_t^{**} is fitted log-differenced discharge; Φ_p are estimated AR parameters operating on the log-differenced discharge series; a_t is a white noise process of random shocks which induce changes in Q_t^*, and θ_q are estimated MA parameters operating on the white noise process in a moving average model. We used an iterative procedure in the computational programming language MATLAB to determine the best univariate model structure for a range of model orders as measured by the autocorrelation and partial autocorrelation functions. A particular model was chosen when the Akaike information criterion (AIC), a measure of the number of model parameters and of the model's fit, was minimized [*Brockwell and Davis*, 1987].

An ARIMA model (5) of the same order was then used to model the output series (i.e., log-differenced sediment concentration). After fitting these ARIMA models separately to the log-differenced discharge and sediment concentration data, the two series of residuals were used for estimating Φ_p and θ_q in (3). *Vandaele* [1983] recommends using these prewhitened series for model identification in order to reflect the true nature of the transfer function model by eliminating all variations in each variable (i.e., log-differenced discharge or sediment concentration) that can be explained by its own past data. These residual data series were then used to estimate the cross-correlation function, ρ_{QCs}, which is a measure of the serial correlation between the two variables Cs and Q, for a given lag k in time (number of days) as

$$\rho_{QCs} = \frac{\gamma_{QCs}(k)}{\sigma_Q \sigma_{Cs}} \qquad k = 0, 1, 2, 3 \ldots, \quad (5)$$

where $\gamma_{QCs}(k)$ is the cross covariance between Q and Cs at lag $+k$ and σ_Q and σ_{Cs} are the standard deviations of the Q and Cs series, respectively. According to a procedure outlined by *Vandaele* [1983], the cross-correlation function aids in identifying some appropriate moving average and autoregressive polynomial orders, ω_s and δ_r, for the transfer function in (3).

We used an iterative, prediction error/maximum likelihood method in MATLAB's System Identification Toolbox [*Ljung*, 1997] to determine the best model structure for a range of model orders suggested by the *Vandaele* [1983] procedure and to minimize the error term in (3). A particular model was chosen from the group of 30 models with the highest model efficiency [*Pierce*, 1979] based on the lowest AIC [*Brockwell and Davis*, 1987]. When choosing between models of similar AIC values, the simpler model (i.e., one with the fewest parameters) was selected. The residuals from the univariate fits were used only for model identification. Once a model structure was identified, the model parameters, ω_s and δ_r in (3), were estimated using the log-differenced series of discharge and sediment concentration without prewhitening. Since the magnitude of model residuals is not known a priori, the noise term is used only for model estimation and is not used in forecasting because the expected value of the model error is zero [*Gurnell and Fenn*, 1984].

After estimating a bivariate model for a particular station, several diagnostic checks were performed to ensure the suitability of the chosen model to represent the physical system

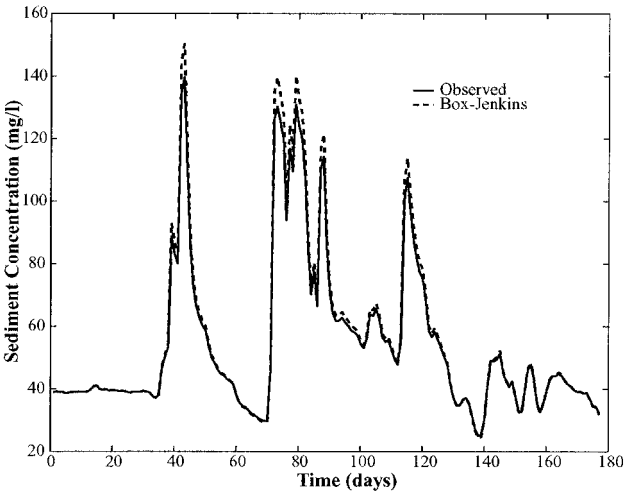

Figure 5. An example of Box-Jenkins (BJ) model predictions versus observed daily values of sediment concentration from a validation data set (not used in model estimation) at the Knights Landing gauging station.

[*Lemke*, 1991]. The autocorrelation of BJ model residuals was plotted to show the absence of serial correlation. The Portmanteau lack-of-fit statistic, which considers groups of residual autocorrelations instead of only individuals, is calculated and must be distributed approximately as χ^2 if the model is appropriate [*Ljung and Box*, 1978]. The cross correlation between the input series (i.e., univariate model residuals of log-differenced discharge) and the bivariate model residuals was examined to check that two were independent. Model stability was assessed by plotting the roots of the characteristic equation on the unit circle. A histogram of the residuals was also plotted to check for a normal distribution. The efficiency of each model, measured by an R^2 coefficient of determination for time series modeling [*Pierce*, 1979], was determined by employing the estimated model to predict sediment concentration on a separate set of validation data. Figure 5 shows an example of model predictions versus the observed validation data in a time series.

6.4. Sediment Budget Calculation

Once a model for a particular station passed all diagnostic tests, it was employed to obtain sediment concentration values over the discharge domain (32 years). The streamflow and modeled sediment concentration were used to calculate daily sediment discharge, S_{day} (in tons), at each main stem gauging station and signature tributary as

$$S_{\text{day}} = Q_{\text{day}} Cs_{\text{day}}, \quad (6)$$

where S_{day} is sediment discharge per day and Q_{day} and Cs_{day} are mean daily discharge and mean daily sediment concentration obtained from the time series analysis, respectively. The S_{day} values for each station were then summed for each water year to obtain S, annual sediment discharge. Long-term average sediment discharge SD for each station was calculated as

$$\overline{\text{SD}} = \left(\sum_{i=1}^{n} S_i \right) \Big/ n, \quad (7)$$

where n is the number of years of record and S_i is the sediment discharge for year i.

The long-term sediment discharge for each tributary was computed from the signature station within the same geologic unit, scaled by a ratio of the drainage areas below any impoundments. The main stem sediment discharge into the unnumbered reach (reach 0) downstream of Shasta Dam (Figure 2) is considered to be zero.

Sediment records for diversions were not extended using BJ models because they are discontinuous (diversions only transport sediment during periods of high flow when the diversion is activated) and thus do not lend themselves to a time series approach. To calculate the sediment efflux from the Sacramento River via major diversions, we used sediment discharge data from the USGS for stations that have it. For one diversion, Glen Colusa Irrigation District (GCID), we have calculated sediment losses into settling ponds using average dredging estimates provided by the GCID. For the remaining major diversions (Anderson Cottonwood Irrigation District and Corning Canal) below Keswick Dam (Figure 2) we have conservatively assumed sediment discharge to be zero.

Long-term suspended sediment discharge divergence for each reach was calculated as

$$S_{\text{div}} = U + T - D - E, \tag{8}$$

where S_{div} is the net sediment divergence for a reach, U is the main stem sediment discharge contribution to the reach from upstream, T is the sum of the discharge contribution to the reach from tributaries, D is the sediment discharge leaving the reach downstream, and E is the sediment efflux via diversions. A suspended sediment budget was thus evaluated for the reaches between the six gauging stations on the main stem Sacramento River.

7. Sediment Budget Results and Discussion

A complete discussion of estimated BJ models is beyond the scope of the present sediment budget analysis, so only main points are mentioned here. Analysis of time series model structures allows for general inferences about the response of sediment concentration to fluctuations in discharge. Although such inferences could be made by analyzing the raw input data used to develop the models, the BJ model quantifies the relationship objectively with simple computation. In the BJ models estimated using (3), there is a preponderance of moving average parameters, indicating a basin responding primarily to fluctuations in discharge with no memory of previous sediment concentration conditions [*Fitzgerald and Karlinger*, 1983; *Lemke*, 1991]. Furthermore, many of the stations' models contain only one estimated parameter indicating that a change in sediment concentration for a given 2-day period is dependent on only the change in discharge for that same period. The models estimated for a few stations have autoregressive terms indicating some persistence in sediment concentration. The R^2 efficiency statistics for all models are very high (see electronic supplement).[1] Models with more parameters were estimated for all stations but resulted in no improvement model efficiency.

[1] Supporting tables are available via Web browser or via Anonymous FTP from ftp://agu.org, directory "apend" (Username = "anonymous", Password = "guest"); subdirectories in the ftp site are arranged by paper number. Information on searching and submitting electronic supplements is found at http://www.agu.org/pubs/esupp_about.html.

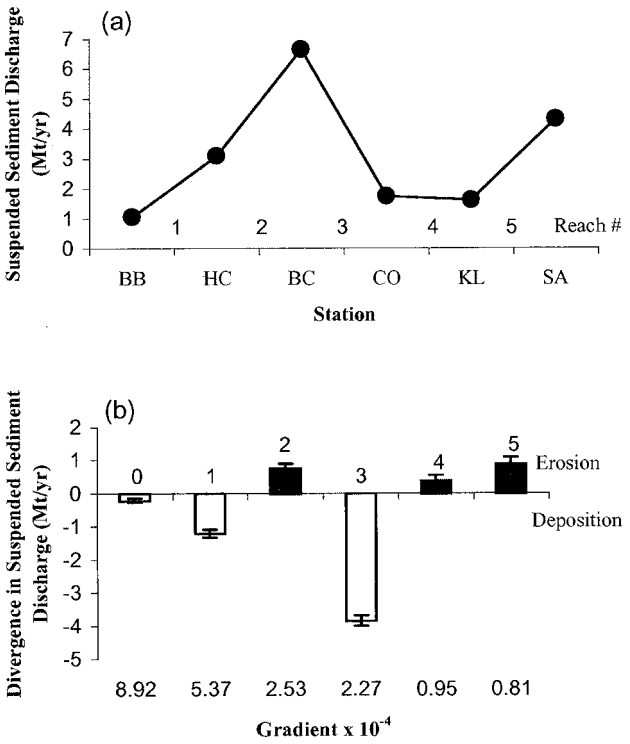

Figure 6. (a) Mean annual sediment flux computed by BJ modeling in millions of tons per year for the six main stem gauging stations, which are denoted on the abscissa by their station abbreviations. The numbers below the curve are the river reach numbers, (b) Sediment flux divergence based on the sediment balance for each reach with the reach gradient on the abscissa. Reach numbers are labeled on the top of each bar.

The sediment budget results are presented in Figure 6 and in the electronic supplement. Figure 6a shows the main stem sediment discharge results derived from BJ modeling at each main stem gauging station. Figure 6b shows main stem sediment discharge divergences for each reach after evaluating the sediment budget. The divergences include the BJ modeling errors that were propogated downstream. Unquantifiable errors associated with input data [*Topping et al.*, 2000] are not included. The spatial patterns of erosion and deposition gleaned from the sediment budget results will be discussed in terms of sediment sources and sinks.

The budget of suspended sediment, including the amount of sediment sequestered in the floodplain, was analyzed for the reach of valley upstream from each of six gauging stations on the main stem Sacramento (Figure 2 and Plate 1). It is important to distinguish this type of analysis from sediment budgets that make determinations about the state of reaches of river channel.

Evaluating the sediment budget using BJ models reveals net deposition in reaches 0, 1, and 3 and net erosion in reaches 2, 4, and 5. The divergences in suspended sediment transport along the main stem Sacramento River appear to be largely the result of tectonic and human influences.

7.1. Deposition in Reach 3

The sediment budget predicts negative divergence in sediment discharge in reach 3, indicating net deposition (Figure

6b). The reach is characterized by a reduction in width from 1830 to 250 m over its 40-km length, while its upstream section contains wide meanders and large sand bars (Figure 3). *Gilbert* [1917] noted that between Colusa and the Feather River confluence (Figure 2), channel capacity of the Sacramento decreased to 10% of its "flood discharge." The reduction in width generally corresponds with two tectonic features. In reach 3 the Sacramento River follows the trace of the Willows Fault toward Colusa. The fault dips steeply to the east and crosses the Sacramento 8 km north of the Colusa gauge. Just over 1 km downstream of Colusa, the river is diverted 2 km eastward for 13 km to traverse Colusa Dome, a southward plunging anticline which displays over 150 m of structural relief on basement rocks [*Harwood and Helley*, 1987]. Although Colusa Dome lacks surface expression, the Sacramento's longitudinal profile shows a decrease in gradient upstream indicating some structural influence or differential compaction of the alluvium over the dome. The interface of the Sacramento River and the dome also corresponds with fixed thalweg elevations associated with the presence of the resistant Modesto Formation outcrop [*WET*, 1990], which was brought to the surface by the dome. It appears that the river migrated away from the Modesto outcrop and incised into softer materials and subsequently became confined to a narrow channel by cohesive, clay-rich banks.

The downstream reduction of width causes water to be sequestered in the wide portions of reach 3 and induces overbank flows and suspended sediment deposition. Sediment is deposited on bars and on the floodplain between setback levees (Figure 3), and $\sim$1.1 Mt yr^{-1} (see electronic supplement) are forced into the floodplain through two flood relief structures which empty into the subsiding Butte Basin (at a rate of $\sim$1.3 mm yr^{-1} [*Ikehara*, 1994]) and Sutter Bypass (Figures 2 and 3). Colusa is the bottleneck of the Sacramento fluvial system because fluxes of water and sediment are diminished at this station (Figure 6b).

7.2. Deposition in Reaches 0 and 1

Although sediment discharge increases between Bend Bridge and Hamilton City (Figure 6a), the sediment budget predicts net deposition of sediment in reaches 0 and 1 (Figure 6b). Reach 0 winds through the steep Sacramento Canyon (slope of 0.0016) below the Keswick Reservoir before reaching the flatter Redding Plain (slope of 0.0011), where the channel is entrenched into a floodplain dissected by the majority of tributaries in reach 0. The Sacramento then enters Iron Canyon before entering the Central Valley above Bend Bridge.

The Redding Plain shows evidence of deposition in the form of point bars (e.g., below Clear and Cottonwood Creeks) as well as tributary fans. The majority of sediment load input to reach 0 of the Sacramento, $\sim$0.5 Mt yr^{-1}, originates in Cottonwood Creek (see electronic supplement). The gauging station used for modeling its sediment load in this study has shown no significant aggradation but is located $\sim$10 km upstream of its confluence with the Sacramento [*McCaffrey et al*., 1988]. The difference between the net increase in sediment transport through the reach and the calculation of net accumulation in the reach is due to massive fan deposition at the confluence and gravel mining which removes large amounts of sand as well as the gravel.

Reach 1 occurs entirely within the Central Valley and has a large, contiguous floodplain separated from the Sacramento River only by natural levees (and occasional riprap). Flood flow, although reduced by Shasta Dam, frequently overtops the natural levees composed of finer sands, silts, and clays [*Brice*, 1977; *WET*, 1990] and causes extensive overbank sedimentation [*Blodgett*, 1971, 1981]. In addition to vertical accretion, lateral floodplain accretion is apparent in this reach in numerous, large sand bars. Another possible location of stored sediments is in the channel of this reach, evident in anomalously fine grain sizes in the bed's subpavement surveyed during low water conditions [*WET*, 1990]. The combination of reduced flood peaks, high tributary input of sediment, and the reduced gradient in the Central Valley ensure net sediment deposition in these reaches.

7.3. Erosion in Reaches 2, 4, and 5

The sediment budget results point to the marked influence of channelization on suspended sediment discharge. The sediment balance at Butte City, Knights Landing, and Sacramento predicts net erosion in these reaches (Figure 6b). We have quantified the average erosion of suspended load from these reaches of river by dividing the flux divergence for each reach by the planform area available for erosion (including banks). This yielded $\sim$1.2 cm yr^{-1}, 0.4 cm yr^{-1}, and 1.7 cm yr^{-1} for reaches 2, 4, and 5, respectively.

In the upper part of reach 2, two major bend cutoffs occurred in 1946, straightening and steepening the channel in the upper part of the reach [*WET*, 1990]. Perhaps as a response to the cutoffs, the minimum thalweg elevation at a cross section below Hamilton City decreased by $\sim$91 cm or $\sim$4.4 cm yr^{-1} between 1949 and 1969 [*WET*, 1990]. It has been shown on the Mississippi River that a wave of channel degradation, associated with increased slope and stream power, travels upstream following natural or anthropogenic cutoff [*Madden*, 1974; *Biedenharn et al*., 2000]. Additionally, *Brice* [1977] observed fewer islands and bars in this reach compared to reach 1. Furthermore, project levees begin at about the halfway point in reach 2, and there are sections where the river is pinned to the levee (Figure 7) leading to locally steep channel gradients and accelerated degradation, as *Kesel and Yodus* [1992] showed along the Mississippi River.

Reach 4, between Colusa and Knights Landing, has no tributaries and has a smaller channel capacity, as floodwaters are attenuated by Butte and Sutter Basins upstream of the bottleneck (i.e., Colusa). This reach has locally steep sections and is a channelized, meandering reach with levees built upon the channel banks. The artificial levees have produced confined bends that concentrate erosion at flow deflections [*Brice*, 1977]. *Biedenharn et al*. [2000] showed that channel confinement on the Mississippi sends a wave of degradation traveling upstream.

Reach 5 continues the pattern of reach 4, with leveed bends, but it is further influenced by the input of water and sediment by Feather River/Sutter Bypass, as well as by Fremont and Sacramento Weirs (Figure 2). Large flood flows leaving the Sacramento through the flood control weirs in this reach cause rapid variations in water surface slope [*Blodgett and Lucas*, 1988] that are capable of inducing erosion. The predicted 1.7 cm yr^{-1} rate of erosion in reach 5 is corroborated in an approximate way by gauge height data from Verona (upstream of the Feather River confluence), which show 42 cm of bed degradation between 1965 and 1979 (3.0 cm yr^{-1}) [*WET*, 1990]. This local erosion is indicative of systemic erosion in the reach, which presumably attenuates downstream with sediment input from the Feather River. Another source of eroded sediment in this reach is the failed leveed banks in the lower Feather River

Figure 7. Aerial photograph showing main channel pinned to west levee (arrow) in reach 2. Levees on the west bank cut off the Sacramento River from Colusa Basin to the west and force overflow into Butte Basin to the east.

(below the gauging station used in this study) and in the lower Sacramento, both of which are consistently the subject of reports evaluating potential for repair and improvement [e.g., *U.S. Army Corps of Engineers*, 1983; *WET*, 1990].

8. Conclusion

Box-Jenkins transfer functions were employed to model the relationship between stream discharge and sediment concentration. Historical records of suspended load were extended over a 32-year period since dam construction on the Sacramento River to analyze spatial patterns in sediment transport. Suspended sediment discharge was calculated, and a sediment budget was evaluated for river reaches between six main stem gauging stations, accounting for their tributaries and diversions. The results of the 32-year sediment budget point to the influence of tectonics and anthropogenic channel modifications on erosion and deposition in the Sacramento Valley.

Notation

a univariate white noise process.
B back shift operator.
Cs sediment concentration, mg L^{-1}.
Cs_{day} mean daily sediment concentration, mg L^{-1}.
d universal delay parameter.
D sediment discharge leaving a reach downstream, t yr^{-1}.
e bivariate error term
E sediment discharge leaving a reach via diversions, t yr^{-1}.
i year index.
k lag, days.
n number of years.
p univariate autoregressive model order.
q univariate moving average model order.
Q discharge, cm.
Q_{day} mean daily discharge, cm.
r bivariate autoregressive polynomial order.
s bivariate moving average polynomial order.
S sediment discharge per year, t.
S_{day} sediment discharge per day, t.
S_{div} net sediment divergence for a reach, t yr^{-1}.
SD long-term sediment discharge, (overbar denotes average) t yr^{-1}.
t current time, days.
T sediment discharge entering a reach from tributaries, t yr^{-1}.
U sediment discharge entering a reach from upstream, t yr^{-1}.
z back shift lag in algebraic notation.
γ cross-covariance function.

δ bivariate autoregressive coefficient.
θ univariate moving average model coefficient.
ρ cross-correlation function.
σ standard deviation.
ω bivariate moving average coefficient.
Φ univariate autoregressive model coefficient.

Acknowledgments. We thank two anonymous reviewers for helpful suggestions which improved the manuscript. Thanks also go to Emmanuel Gabet and Daniel Malmon for comments on earlier versions of the manuscript and to Randy Singer for statistical assistance and suggestions on improving figure presentation. We would also like to acknowledge the support of NASA grant NAG5-6120.

References

Biedenharn, D. S., C. R. Thorne, and C. C. Watson, Recent morphological evolution of the Lower Mississippi River, *Geomorphology*, *34*, 227–249, 2000.

Blodgett, J. C., Determination of floodflow of the Sacramento River at Butte City, California, January 1970, *U.S. Geol. Surv. Open File Rep*., *72-40*, 1971.

Blodgett, J. C., Floodflow characteristics of the Sacramento River in the vicinity of Gianella Bridge, Hamilton City, California, *U.S. Geol. Surv. Open File Rep*., *81-328*, 1981.

Blodgett, J. C., and J. B. Lucas, Profile of Sacramento River, Freeport to Verona, California, flood of February 1986, *U.S. Geol. Surv. Open File Rep*., *88-82*, 1988.

Box, G., and G. Jenkins, *Time Series Analysis, Forecasting, and Control*, Holden Day, San Francisco, Calif., 1994.

Brice, J., Lateral migration of the middle Sacramento River, California, *U.S. Geol. Surv. Water Resour. Invest. Rep*., *77-43*, 1977.

Brockwell, P., and R. Davis, *Time Series: Theory and Methods*, 519 pp., Springer-Verlag, New York, 1987.

Bryan, K., Geology and groundwater resources of Sacramento Valley, California, *U.S. Geol. Surv. Water Supply Pap*., *495*, 1923.

California Department of Water Resources, Sacramento River bank erosion investigation, progress report, Sacramento, Calif., 1994.

Dendy, F. E., and W. A. Champion, Sediment deposition in US reservoirs: Summary of data reported through 1975, *Misc. Publ*. *1362*, U.S. Dep. of Agric., Washington, D. C., 1978.

Dunne, T., Geomorphologic contributions to flood control planning, in *Flood Geomorphology*, edited by V. R. Baker, R. C. Kochel, and P. C. Patton, pp. 421–438, John Wiley, New York, 1988.

Ferguson, R. I., River loads underestimated by rating curves, *Water Resour. Res*., *22*(1), 74–76, 1986.

Fitzgerald, M. G., and M. R. Karlinger, Daily water and sediment discharges from selected rivers of the eastern US: A time series modeling approach, *U.S. Geol. Surv. Water Supply Pap*., *2216*, 1983.

Gilbert, G. K., Hydraulic-mining debris in the Sierra Nevada, report, U.S. Geol. Surv., Menlo Park, Calif., 1917.

Goodwin, P., and R. A. Denton, Seasonal influences on the sediment transport characteristics of the Sacramento River, California, *Proc. Inst. Civ. Eng*., *91*, 163–172, 1991.

Gurnell, A. M., and C. R. Fenn, Box-Jenkins transfer function models applied to suspended sediment concentration-discharge relationships in a proglacial stream, *Arct. Alp. Res*., *16*(1), 93–106, 1984.

Guy, H. P., and V. W. Norman, Field methods for measurement of fluvial sediment, *U.S. Geol. Surv. Tech. Water Resour. Invest*., *Book 3*, *Chap. C2*, 59 pp., 1970.

Harwood, D. S., and E. J. Helley, Late Cenozoic tectonism of the Sacramento Valley, California, *U.S. Geol. Surv. Prof. Pap*., *1359*, 1987.

Heidel, S. G., The progressive lag of sediment concentration with flood waves, *Eos Trans*., *AGU*, *37*(1), 56–66, 1956.

Ikehara, M. E., Global positioning system surveying to monitor land subsidence in Sacramento Valley, CA, USA, *Hydrol. Sci*., *39*(5), 417–429, 1994.

James, L. A., Incision and morphologic evolution of an alluvial channel recovering from hydraulic mining sediment, *Geol. Soc. Am. Bull*., *103*, 723–736, 1991.

Kesel, R. H., and E. G. Yodus, Some effects of human modifications on sand-bed channels in southwestern Mississippi, USA, *Environ. Geol. Water Sci*., *20*(2), 93–104, 1992.

Kesel, R. H., E. G. Yodis, and D. J. McCraw, An approximation of the sediment budget of the lower Mississippi River prior to major human modification, *Earth Surf. Processes Landforms*, *17*(7), 711–722, 1992.

Kondolf, G. M., Geomorphological stream channel classification in aquatic habitat restoration: Uses and limitations, *Aquat. Conserv. Mar. Freshwater Ecosyst*., *5*, 127–141, 1995a.

Kondolf, G. M., Managing bedload sediment in regulated rivers: Examples from California, USA, in *Natural and Anthropogenic Influences in Fluvial Geomorphology: The Wolman Volume*, *Geophys. Monogr. Ser*., vol. 89, edited by J. E. Costa et al., pp. 165–176, AGU, Washington, D. C., 1995b.

Kondolf, G. M., and M. G. Wolman, The sizes of salmonid spawning gravels, *Water Resour. Res*., *29*(7), 2275–2285, 1993.

Lemke, K., Transfer function models of suspended sediment concentration, *Water Resour. Res*., *27*(3), 293–305, 1991.

Ljung, G. M., and G. E. P. Box, On a measure of lack of fit in time series models, *Biometrika*, *65*(2), 297–303, 1978.

Ljung, L., *System Identification Toolbox User's Guide*, Mathworks, Inc., Natick, Mass., 1997.

Loughran, R. J., The calculation of suspended-sediment transport from concentration v. discharge curves: Chandler River, N.S.W., *Catena*, *3*, 45–61, 1976.

Madden, E. B., Mississippi River and Tributaries Project, Problems relating to changes in hydraulic capacity of the Mississippi River, *USACE Rep*., *TR 12*, U.S. Army Corps of Eng., Vicksburg, Miss., 1974.

Marcus, A. W., Lag-time routing of suspended sediment concentrations during unsteady flow, *Geol. Soc. Am. Bull*., *101*, 644–651, 1989.

McCaffrey, W. F., J. C. Blodgett, and J. L. Thornton, Channel morphology of Cottonwood Creek near Cottonwood, Calif. from 1940 to 1985, *U.S. Geol. Surv. Water Resour. Invest. Rep*., *87-4251*, 1988.

Meade, R. H., Sources, sinks, and storage of river sediment in the Atlantic drainage of the United States, *J. Geol*., *90*, 235–252, 1982.

Neter, J., W. Wasserman, and M. Kutner, *Applied Linear Regression Models*, 547 pp., Richard D. Irwin, Homewood, Ill., 1983.

Pierce, D. A., R^2 measures for time series, *JASA J. Am. Stat. Assoc*., *74*(368), 901–910, 1979.

Porterfield, G., *Computation of Fluvial-Sediment Discharge*, *U.S. Geol. Surv. Tech. Water Resour. Invest*., *Book 3*, *Chap. 3*, 66 pp., 1972.

Porterfield, G., Sediment transport of streams tributary to San Francisco, San Pablo, and Suisun Bays, California, 1909–66, *U.S. Geol. Surv. Water Resour. Invest. Rep*., *80-64*, 1980.

Rodriguez-Iturbe, I., and C. F. Nordin, Time series analyses of water and sediment discharges, *Hydrol. Sci. J*., *13*(2), 69–84, 1968.

Sharma, T., and W. Dickinson, System model of daily sediment yield, *Water Resour. Res*., *16*(3), 501–506, 1980.

Sharma, T. C., W. G. S. Hines, and W. T. Dickinson, Input-output model for runoff-sediment yield processes, *J. Hydrol*., *40*, 299–322, 1979.

Topping, D. J., D. M. Rubin, and J. L. E. Vierra, Colorado River sediment transport, 1, Natural sediment supply limitation and the influence of Glen Canyon Dam, *Water Resour. Res*., *36*(2), 515–542, 2000.

U.S. Army Corps of Engineers, Sacramento River and tributaries bank protection and erosion control investigation, California, report, Sacramento, Calif., 1983.

Vandaele, W., *Applied Time Series and Box-Jenkins Models*, 417 pp., Academic, San Diego, Calif., 1983.

Walling, D. E., Assessing the accuracy of suspended sediment rating curves for a small basin, *Water Resour. Res*., *13*(3), 531–538, 1977.

Water Engineering and Technology, (WET), Geomorphic analysis of Sacramento River, Phase II report, Fort Collins, Colo., 1990.

Williams, G. P., Sediment concentration versus water discharge during single hydrologic events in rivers, *J. Hydrol*., *111*, 89–106, 1989.

T. Dunne and M. B. Singer, Donald Bren School of Environmental Science and Management, University of California, Santa Barbara, Santa Barbara, CA 93106, USA. (tdunne@bren.ucsb.edu; bliss@bren.ucsb.edu)

(Received February 26, 2001; revised August 27, 2001; accepted August 30, 2001.)